Proceedings of the 2017 Winter Simulation Conference
W. K. V. Chan, A. D'Ambrogio, G. Zacharewicz, N. Mustafee, G. Wainer, and E. Page, eds.

HYBRID AGENT-BASED MODELING OF ZIKA IN THE UNITED STATES

Chris J. Kuhlman
Yihui Ren
Bryan Lewis
James Schlitt

Biocomplexity Institute
Virginia Tech
1015 Life Science Circle
Blacksburg, VA 24061, USA

ABSTRACT

Vector-borne infectious diseases present computational modelers with a unique challenge: finding the right balance between model fidelity and simulation costs. In this work, we introduce a hybrid agent-based model that achieves a balance that readily scales to problem sizes of millions of human agents and mosquitoes. Macroscopically, our model results agree with those from a low-cost compartmental model; microscopically, like agent-based models, it provides details at the individual level. We apply this model to a synthetic human population of 1.2 million individuals from Miami, Florida in the United States to model the Zika outbreak in the Fall of 2016. We identify two high-risk locations within this region, a detail which cannot be revealed by traditional compartmental models. The principles-based mathematical derivation of the hybrid agent-based model can be adapted to other scenarios facing similar tradeoffs.

1 INTRODUCTION

1.1 Background and Motivation

Vector-borne diseases account for one sixth of all cases of infectious human diseases. Throughout history, the control of some of these diseases has been among the greatest public health successes (e.g. malaria elimination in the US, yellow fever elimination in the Americas). However, as the world has become increasingly more interconnected and urbanized, and as the impact of climate change becomes more apparent, the threat of these diseases will become more pronounced.

Mosquito-borne diseases can spread rapidly, with chikungunya reaching 75% of the population of Lamu, Kenya, Africa in 2004 (Sergon et al. 2009). In Summer 2014, Zika was detected in Brazil and spread through Latin America at startling speed, sweeping across the South American continent in two years, causing significant morbidity and mortality. During 2016 alone, Zika spread through some 47 countries and territories (Zhang et al. 2017), and was declared a public health emergency by the World Health Organization. The first known cases of Zika transmission from mosquitoes to humans in the U. S. occurred in Miami, Florida in the Fall of 2016. Although Zika can spread human-to-human through sexual contact and to a baby in the womb, Zika spreads primarily through contact with infected mosquitoes (Chouin-Carneiro et al. 2016). Consequently, much work has been devoted to understanding Zika, including its transmission using agent-based modeling (Gu and Novak 2009), compartmental models (Gu and Novak 2009), and other approaches (Perkins et al. 2016).

Ordinary differential equation (ODE)-based and agent-based models (ABM) are commonly used to simulate the spread of infectious diseases. ODE or compartmental models run relatively quickly but are not informative at the individual level; ABMs provide individual level granularity, but simulations are expensive

to run. Vector-borne infectious diseases, such as Zika, present a unique challenge for simulation. High fidelity models (ABMs) enable more realistic policy planning; however, simulating each mosquito as an agent is computationally challenging. Agent-based simulations (ABSs) that incorporate individual mosquito behavior have typically been limited to a couple of thousand mosquitoes (e.g., Jindal and Rao (2017)), which is not suitable for large populations over large geographic regions. To address these competing considerations, we introduce a hybrid ABM (HABM) in which an ABM captures individual human behavior and gridcells contain ODE models that capture mosquito behavior. Our model provides a desirable balance between computational cost and model fidelity. This approach also enables the incorporation of high fidelity mobility of agents.

1.2 Contributions

Our central focus is a process of converting a compartmental model to an HABM, and comparison of results between the two models. However, we also illustrate its use and value by modeling an actual Zika outbreak in the United States. The major contributions of this work follow.

1. Principled method for converting a compartmental model to a hybrid agent-based model (HABM). Our starting point is the compartmental model of (Manore et al. 2014), in which there is one compartment for humans and one for a gridcell that contains mosquitoes. Disease transition is mosquito-to-human and human-to-mosquito. We provide a principled process, in the form of model equations, to convert from a compartmental model to a HABM. We use a conversion process based on the harmonic mean of the forces of infection from Manore et al. (2014), which is essentially a transmission kernel. While we apply this model to Zika, we expect the HABM to have wider applicability, to other vector- and mosquito-borne diseases such as Dengue and Chikungunya.

2. Comparison of HABM and compartmental model results. HABM results are compared against compartmental model results from (Manore et al. 2014), where each simulation spans eight years of system (disease) dynamics for a 100,000-member human population and 200,000 mosquitoes. We provide results for Denge [DENV (Aedes aegypti)] and Chikungunya [CHIK-R (Aedes albopictus)].

3. Application of the HABM to realistic scenarios of Zika outbreaks in Miami, Florida. In the late Summer/early Fall of 2016, the first instance of autochthonous transmission of Zika virus via mosquitoes in the United States was observed in Miami, Florida. From the initial seed of a returning international traveler, mosquitoes in Miami became infected, and from there transmission continued for several months, before eventually being brought under control. Ultimately, among more than one million residents, over 200 instances of transmission occurred in Miami via mosquitoes. We calibrate our model to these data and then perform additional simulations to understand Zika dynamics.

Paper organization. Section 2 contains related work. Section 3 on modeling contains an overview of the compartmental model (Manore et al. 2014) that is the starting point for our work; an overview of our HABM; comparisons of results between our HABM and the compartmental model (Manore et al. 2014); and a short description of the Miami population. Section 4 contains results from simulations of Zika outbreaks in Miami. The paper concludes with Section 5, including limitations of this work.

2 RELATED WORK

Viana (2014) states that hybrid simulation is typically the combination of discrete event simulation (DES), systems dynamics (SD), and agent-based models (ABM). SD methods include compartmental models and ODE-based models. DES is the control methodology (based on events) for invoking ABMs. Consequently, often DES and ABM are combined in that DES is one approach for scheduling execution of ABMs (another being discrete time simulation). Here, we combine discrete time simulation (DTS) and agent models, and refer to this as agent-based simulation (ABS) and ABM. Hybrid simulation is used in many domains such

as construction, energy systems, chemical engineering, social modeling, healthcare, and biology (Viana 2014).

There are two dimensions along which to combine ABM and DS: (i) level of aggregation/disaggregation, and (ii) time evolution. DS typically involves aggregated models and continuous time. ABM typically involves disaggregated models and discrete time or events.

Three modes of DES and DS interactions are cited in Chahal and Eldabi (2008): (i) *hierarchical* where two distinct models pass data to one another, (ii) *process environment* where a DES models sits within an SD model and interacts with it cyclically, and (iii) *integrated* where there is one model with no clear distinction between the discrete and continuous parts. This breakdown is somewhat difficult to operationalize because it includes particular uses of the SD and ABM models. For example, the first class is for the case where SD models are used at the strategic level, while ABM (or DES) is used at the operational level, which specifies the *use* of each paradigm.

Brailsford et al. (2010) states that a "genuinely hybrid model switches back and forth between continuous and discrete models." We use hybrid modeling in the sense of Brailsford et al. (2010): we execute a discretized version of a continuous compartmental model and discrete ABMs simultaneously within a distributed, parallel simulation system. There are many other hybrid approaches; see Chahal and Eldabi (2008), Schweitzera and Garcia (2010), Viana (2014), Schwarz and Pruyt (2016). In the healthcare model of Mielczarek and Zabawa (2016), an SD scheme is used to age a population. An ABM is used to spread a disease through the aged population to estimate human loads on hospitals. Information flow is one-way, from SD to ABM as people age, but this data movement occurs a multitude of times. In some hybrid models, interactions between entities may take place in only one type of model; e.g., only in the ABM (Mielczarek and Zabawa 2016)or only in the SD model (Viana 2014). In contrast, our HABM has entity interactions in both the ABM [humans] and the SD (i.e., ODE) model [mosquitoes], and between entities across the model types so that information flows in both directions.

There are works that compare SD and ABM results for the same phenomena. However, most are like Figueredo et al. (2014) in that the two models (SD and ABM) are developed independently, and results are compared. Here, we are doing something different: we are *converting* an SD model to a HABM to achieve greater granularity in model outputs.

The work closest to ours is that of Manore et al. (2015). They also use individual agents to represent humans and compartments to represent collections of mosquitoes for vector-borne diseases. However, there are many differences. Our population is orders of magnitude larger (1.2 million vs. 1,500 people and 10,000 vs. 3 compartments for mosquitoes). Our population is a synthetic representation of the Miami-Dade County area of FL vs. limited realistic data. Our resulting network is a bipartite graph of people visiting locations/gridcells (more in Section 3.4) based upon the aforementioned synthetic population, whereas theirs is an Erdos-Renyi random network. We provide a much more realistic case study: the Fall 2016 Zika outbreak in Miami, FL. We describe *how* the compartmental model is converted to an HABM. We perform computations with our HABM and compare results with those from the ODE model.

3 METHODS

This section consists of a description of the compartmental model (3.1), a description of the HABM (3.2), comparisons of results from the two models (3.3), and an overview of the population model that is used in the simulations (3.4).

Two views of the high level model setups are shown in Figure 1. At the top of Figure 1a is the compartmental model with two compartments, all humans and all mosquitoes, per Manore et al. (2014). This model is converted, in this work, to an HABM as described in the lower portion of Figure 1a. In Figure 1b, the states and transitions of mosquitoes and humans are provided. Note that humans only get infected from interactions with mosquitoes, and vice versa. That is, there is no human-to-human transmission in this model.

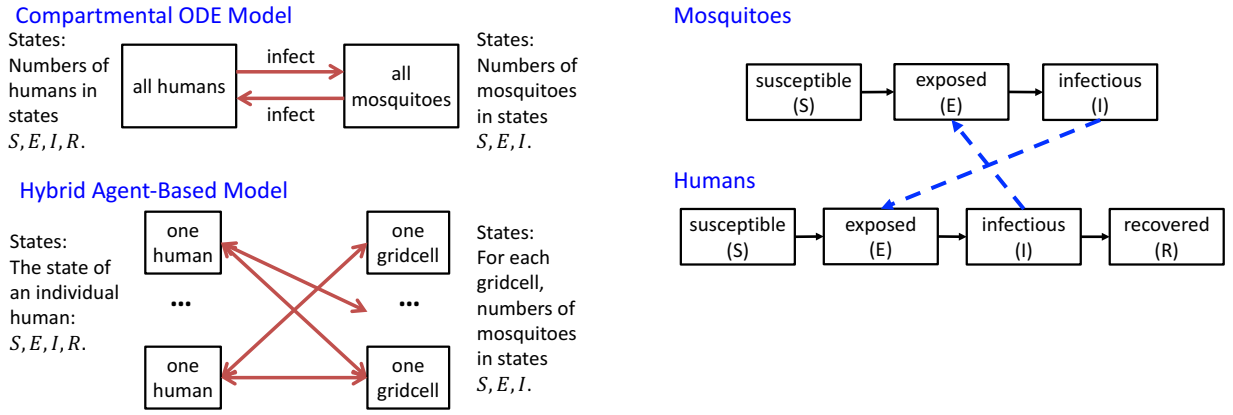

(a) (b)

Figure 1: (a) [top] Compartmental (or patch or ODE) model view of Manore et al. (2014), and [bottom] the hybrid ABM view used here. In the compartmental view, there are two compartments: one for humans and one for mosquitoes. States are *counts* of agents in each state (S, E, I, R for humans) and (S, E, I for mosquitoes). In the HABM, each human is an individual agent, so the state of an agent is one of (S, E, I, R). Also in the HABM, each gridcell is an agent. Each gridcell agent contains a collection of mosquitoes, as in the compartmental model. This means that states for a gridcell remain *counts* of mosquitoes in states (S, E, I). (b) The state machines for each of mosquitoes and humans. The state sets of mosquito and human agents both include S, E, and I, and the human agent also includes R. Humans and mosquitoes transfer virus when each is infectious (dashed blue lines), causing the recipient to transition to the E state (i.e., infected, but not yet infectious). In particular note that humans do not infect each other in this model.

3.1 Compartmental Model

Time-dependent ODEs are used to describe the evolution of a dynamical system. Individuals are grouped into compartments based on their states. For example, the SEIR epidemic model for humans in the Zika model contains four compartments: susceptible, exposed, infectious, and recovered. The numbers of individuals in different compartments are defined as time-dependent macroscopic *variables*, vector $\boldsymbol{v}$, i.e. $\boldsymbol{v} = \{S, E, I, R\}$. Therefore, ODE models in epidemiology are also known as compartmental models. To capture the temporal evolution of the dynamical system, ODE models also define a set of *parameters* a_{ij} as the rate of change from state j to state i (a_{ij} could be zero). Then, the dynamical system can be expressed as a system of ODEs: $\dot{\boldsymbol{v}} = \boldsymbol{A}\boldsymbol{v}(t)$, with $a_{ij} \in \boldsymbol{A}$.

There are many ways of extending ODE models. If individuals in a dynamical system form distinctive groups (i.e. vector-host or male-female), we can subdivide the SEIR compartments into finer compartments. For example, in the study of vector-borne infectious disease modeling (Manore et al. 2014), human (subscript h) and mosquito (subscript v as in vector-borne) naturally form two different groups. The compartments of the dynamical system are then $\boldsymbol{v} = \{S_h, E_h, I_h, R_h, S_v, E_v, I_v\}$.

Due to space limitations, we focus on two ODEs of most interest—those involving interactions between humans and mosquitoes, depicted as blue dashed lines in Figure 1b:

$$\frac{dE_h}{dt} = \lambda_h(t)S_h - \nu_h E_h - \mu_h E_h \qquad \text{and} \qquad \frac{dE_v}{dt} = \lambda_v(t)S_v - \nu_v E_v - \mu_v E_v\,, \tag{1}$$

where ν is the rate of transition to the infectious state I; μ is the death rate; and λ_h (and λ_v) is called the *force of infection*, describing the rate of change of human (mosquitoes) from S to E due to contact with infectious mosquitoes (humans). Explicitly, λ_h and λ_v are written as follows:

$$\lambda_h = \frac{1}{N_h} b \beta_{hv} \frac{I_v}{N_v} , \qquad \lambda_v = \frac{1}{N_v} b \beta_{vh} \frac{I_h}{N_h} , \qquad \text{and} \qquad b \equiv \frac{\sigma_v N_v \sigma_h N_h}{\sigma_v N_v + \sigma_h N_h} , \tag{2}$$

where β_{hv} is the probability of transmission per bite from v to h; σ_v is the maximum number of times one mosquito bites a human per unit time; and σ_h is the maximum number of mosquito bites a human can sustain per unit time. $N_v(t)$ is the number of mosquitoes in a compartment at time t; and $N_h(t)$ is the number of humans in a location compartment at time t. Note that the value b in (2), the total contacts between humans and mosquitoes, is a harmonic mean of the contributions from mosquito and human compartments. Force of infection λ is proportional to b and infectious fraction I/N, with a unit of per unit time per capita.

3.2 Hybrid Agent-Based Model

In our HABM, an individual human is represented as an agent in an ABM; mosquitoes are confined to regions that are represented as compartments; see the lower part of Figure 1a. Since our compartments will represent geospatial regions of a grid, we call the compartments *gridcells*. (This will be described in Section 3.4.) Each individual human follows a travel schedule, presenting herself at a particular gridcell during a certain time interval. The variable subscript h now indicates a particular human individual, instead of a human compartment. As there are multiple gridcells, we change the variable subscript of mosquito compartment from v to g (for gridcell); e.g., I_g represents the total number of infectious mosquitoes in gridcell g. We also introduce a binary indicator $\hat{N}_{hg}(t) \in \{0,1\}$: 1 if human h is at gridcell g at time t; 0 otherwise.

The main issue in developing the HABM from the compartmental model is to convert the mathematical expressions of compartment-compartment interactions to agent-compartment interactions; in particular, the forces of infection in (2). The total number of contacts b at gridcell g depends on the set of individuals visiting gridcell g at time t and σ_h (maximum bites sustained per unit time) of each particular individual in g at t. We can express the total number of contacts b at gridcell g at time t as:

$$b_g(t) = \frac{\sigma_g N_g (\sum_{h=1}^{N_h} \sigma_h \hat{N}_{hg}(t))}{\sigma_g N_g + \sum_{h=1}^{N_h} \sigma_h \hat{N}_{hg}(t)} , \tag{3}$$

where the summands in each summation are *individual* human attributes. Compare this result to that in (2). Therefore, the forces of infection $\lambda_h(t,g)$ (from mosquitoes at gridcell g to a human h) and $\lambda_g(t)$ are:

$$\lambda_h(t,g) = \frac{1}{N_{hg}(t)} b_g(t) \beta_{hg} \frac{I_g(t)}{N_g(t)} \qquad \text{and} \qquad \lambda_g(t) = \frac{1}{N_g(t)} b_g(t) \bar{\beta}_{gh} \frac{I_{hg}(t)}{N_{hg}(t)} , \tag{4}$$

where $N_{hg}(t) = \sum_{h=1}^{N_h} \hat{N}_{hg}$ is the total number of humans at gridcell g; and $I_{hg}(t) = \sum_{h=1}^{N_h} \hat{I}_h \hat{N}_{hg}$ is the total number of infectious humans at gridcell g and $\hat{I}_h = 1$ if human h is infectious. β_{hg} has the same meaning as β_{hv} except it is regarding a particular human agent instead of a human compartment. $\bar{\beta}_{gh}$ is the average transmission rate of all human agents at gridcell g weighted by their individual σ_h; i.e., $\bar{\beta}_{gh} = \sum_{h=1}^{N_h} \sigma_h \beta_{gh} \hat{N}_{hg}(t) / \sum_{h=1}^{N_h} \sigma_h \hat{N}_{hg}(t)$. These summations are over individuals that can be assigned individual properties. Moreover, if the number of humans in a gridcell changes per time unit, for example, then parameters like $\bar{\beta}_{gh}$ will change in time.

We can express our model explicitly as two parts: ABM for humans and (discrete-time) ODE for gridcells of mosquito (compartments). For a human agent, as with a conventional ABM, to determine whether it changes from one state to another, we generate a random number $q \in [0,1]$, and compare it with the corresponding state transmission rate. The rate from S to E depends on the time and gridcell, whereas

other rates are constant. We have

$$\Pr(S_h \to E_h | g,t) = \begin{cases} 1, & q < \lambda_h(t,g) \\ 0, & \text{otherwise}, \end{cases} \quad (5)$$

$$\Pr(E_h \to I_h) = \begin{cases} 1, & q < \nu_h \\ 0, & \text{otherwise}, \end{cases} \quad (6)$$

$$\text{and} \quad \Pr(I_h \to R_h) = \begin{cases} 1, & q < \gamma_h \\ 0, & \text{otherwise}. \end{cases} \quad (7)$$

For a gridcell (mosquito compartment), we use a system of ODEs given by

$$S_g(t) = S_g(t-1) - \underbrace{\lambda_g(t) S_g(t-1)}_{\text{trans. to } E} - \underbrace{\mu_g S_g(t-1)}_{\text{deaths}} + \underbrace{h_g(N_g) N_g}_{\text{births}}, \quad (8)$$

$$E_g(t) = E_g(t-1) + \underbrace{\lambda_g(t) S_g(t-1)}_{\text{trans. from } S} - \underbrace{\nu_g E_g(t-1)}_{\text{trans. to } I} - \underbrace{\mu_g E_g(t-1)}_{\text{deaths}}, \text{ and} \quad (9)$$

$$I_g(t) = I_g(t-1) + \underbrace{\nu_g E_g(t-1)}_{\text{trans. from } E} - \underbrace{\mu_g I_g(t-1)}_{\text{deaths}}, \quad (10)$$

where S_g, E_g, and I_g are the counts of susceptible, exposed, and infectious mosquitoes in gridcell g. Our model does not take into account mosquito mobility from one gridcell to another; this is part of our future work.

3.3 Comparisons of Results Between the Compartmental Model and the HABM

Each compartmental model-based simulation in Manore et al. (2014) consists of one compartment containing 200,000 mosquitoes and one compartment with 100,000 humans. In each case, one human is prescribed as initially infected; all other humans are initially in the susceptible state S and all mosquitoes are also initially in the susceptible state. We simulate the same scenarios using the HABM, with 100,000 individual human agents and one gridcell with 200,000 mosquitoes. For each HABM simulation, we ran 30 runs or instances, where a simulation instance consists of specifying initial conditions at time $t = 0$ and running the simulation in discrete time, by day, to time $t_{max} = 8$ years, consistent with Manore et al. (2014). For each run, one human agent was selected uniformly at random to be the *seed*; i.e., the agent that is initially infected. The HABM simulations compute all agents states at the end of each day over the eight years. All property values used in Manore et al. (2014) were also used in the HABM; properties are the variables in Section 3.2. Figure 2 shows good agreement in results for the two types of models.

3.4 Synthetic Population of Central Miami, FL

A synthetic population and social network of Miami, Florida in the United States were constructed. The population generation process creates a population of representative human agents and assigns attributes to them (e.g., age, gender, household structure, home location) (Barrett et al. 2009, Bisset et al. 2016). Each person is assigned a daily activity pattern, consisting of two or more activities. Locations of the person's activities are assigned based on her home location and based on land use surveys for building types. We restrict the population model to the urban downtown region of Miami that includes the Atlantic Coast and Miami Beach, and we call this *Central Miami*. There are 1,246,818 people that live or have activities in Central Miami. Each person can have activities within the six categories of home, work, school (for youth), college (for older students), shopping, and other. This population has 1,817,966 daily home activities and 2,306,586 daily activities outside of the home—this is a *normative* day. A person visits locations that correspond to their daily activities.

Central Miami area is divided into a 100×100 grid (for a total of 10^4 gridcells). Each gridcell is labeled with its latitude-longitude coordinate and is assigned a number of mosquitoes. Locations (for human activities) are situated within gridcells. Thus, when a person visits a location, she is also visiting a

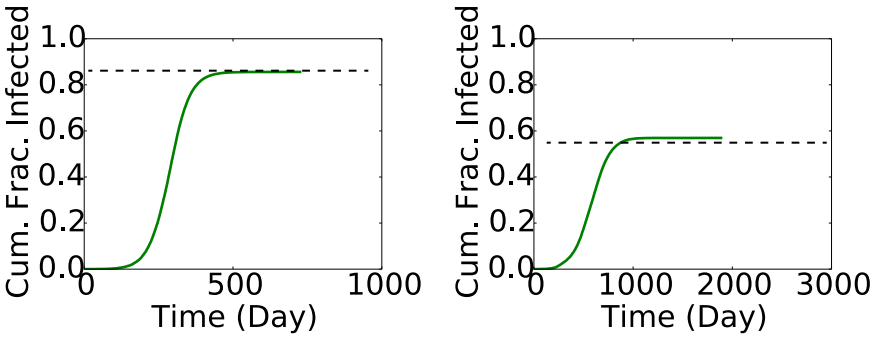

(a) (b)

Figure 2: Comparison of HABM results (solid curves) and compartmental model results (dashed curves) for (a) a dengue DENV (Aedes aegypti) outbreak, and (b) a chungunya (CHIK-R) (Aedes albopictus) outbreak, each on a 100,000-person and 200,000-mosquito population. Each human is an individual agent in the HABM and, for this comparison, each simulation uses only one compartment for the mosquito populations. Computations are of human and mosquito disease states on a daily basis for eight years. Each plot shows the cumulative fraction of humans that have been infected, in time. The peak values in the curves, time-to-peak, and shape of the curves are in good agreement with those from the compartmental model of Manore et al. (2014); the peak values from the compartmental models are shown as horizontal dashed lines.

gridcell. Figure 3a is a heatmap of human-day density within the gridcells of Central Miami, and gives an indication of the amount of human traffic in each cell: the greater the intensity, the more human-days are spent in the region. Figure 3b shows that the population within the gridcells is approximately lognormally distributed.

4 SIMULATIONS AND RESULTS

4.1 Simulation Description

A series of simulations of Zika transmission in Central Miami, Florida have been performed to evaluate our HABM. Inputs to a simulation consist of the 1.25M individual human agents; the 100×100 gridcells containing mosquito populations and the locations that humans visit during their normative days; and the property values of the parameters in the model of Section 3.2. We used in our HABM all of the property values used in (Manore et al. 2014), in their Table 3, for DENV (Aedes aegypti), except that in (Manore et al. 2014), $\beta_{gh} = \beta_{hg} = 0.33$ (labelled β_{vh} and β_{hv}, respectively, in that work). Here, we calibrate $\beta_{gh} = \beta_{hg}$ as described below, but we keep these two parameter values the same, following (Manore et al. 2014). We assume that there are initially two mosquitoes for every human that visits or resides in a building within that gridcell, also following Manore et al. (2014). If an infectious human is bitten by a susceptible mosquito and the mosquito contracts Zika, then it can transfer the virus to other humans that visit the same or other locations within that gridcell if it bites them. There is no human-to-human transmission; only human-to-mosquito and mosquito-to-human. The latter transmission types are the dominant ones; human-to-human transmission is comparatively small (Chouin-Carneiro et al. 2016). Each visit to a location within a gridcell has begin and end times, and these visit durations are accounted for in the HABM of Section 3.2, so that visits of humans to locations in gridcells are specified in granularity of seconds.

A **simulation instance** or **run** begins at time $t = 0$ with a number n_s of initially infected humans, selected uniformly at random from the Wynwood area of Central Miami, where the actual outbreak started. We focus on $n_s = 1$ and 10. There are no infected mosquitoes initially; all are susceptible. From the initial human infection(s), either mosquitoes in some gridcells are infected when they bite the initially infected

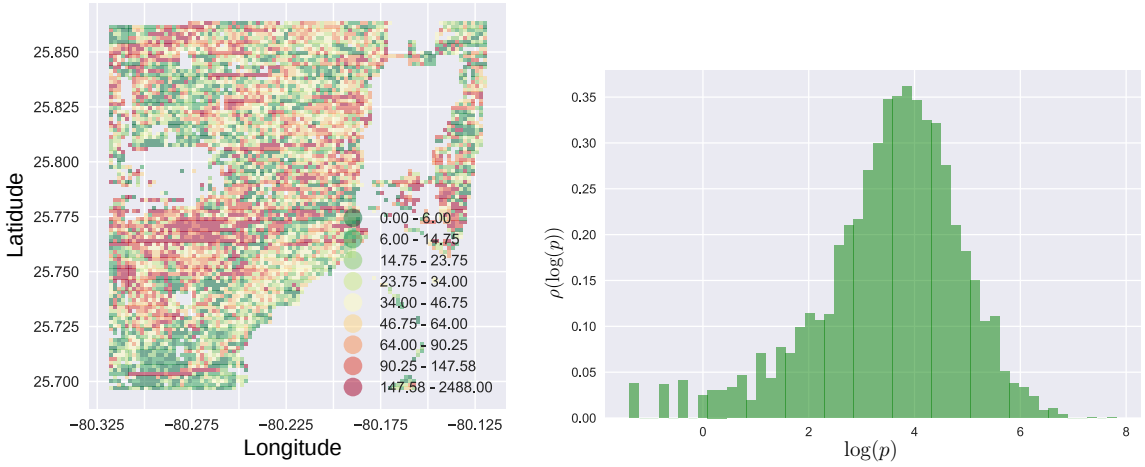

(a) (b)

Figure 3: (a) The spatial distribution of total human time spent in the gridcells of the urban downtown area of Miami, FL near the coast, which we call Central Miami. The data are the number of human-days spent in each gridcell, on a normative day. For example, if two people each spend 6 hours in one gridcell on a normative day, this is 12 hours or 0.5 human-days. (b) The histogram of the logarithm of the human-days p at each gridcell of Central Miami.

people, or no mosquitoes are infected. In the latter case, the virus transmission terminates. Each human makes daily visits to its assigned locations (and gridcells) at the prescribed times, and states are updated according to Section 3.2. At the end of each day, the state of each human agent (S, E, I, or R) is recorded, as are the numbers of mosquitoes in states S, E, and I in each gridcell. In all cases, we simulate for $t_{max} = 60$ days of the Zika outbreak in Central Miami in the Fall of 2016. A **simulation** is a set of 50 simulation instances, whose runs differ in the randomly selected seed nodes.

Simulation studies overview. The sections on results below are organized as follows. First, results from a calibration exercise are provided, where we use all Zika model properties from Manore et al. (2014) except that we calibrate β_{gh} and β_{hg} to reproduce the number of observed Zika infections in Central Miami in Fall 2016. Second, the results of spatial spreading of Zika are presented. Third, we compare spatial spreading of Zika for more aggressive human-mosquito transmission. We also illustrate how these results provide additional insights over compartmental models. Finally, we provide results for illustrative interventions.

4.2 Calibration and Time Histories for Central Miami Outbreak in Fall 2016

We performed a calibration exercise where we systematically varied $\beta_{gh} = \beta_{hg}$ from 0.20 to 0.36 to reproduce the number of infected in an actual outbreak: 120 infected humans in Central Miami over a 2-month period in Fall 2016. These infections emanated from one initially infected individual in the Wynwood area of Central Miami. We found that $\beta_{gh} = \beta_{hg} = 0.274$ produced 120 infected people, on average, over 50 runs.

Figure 4 contains results for the baseline Central Miami simulation of this outbreak. Figure 4a contains the so-called epi-curves for 50 instances in black, with the average curve in magenta. Figure 4b contains the cumulative fraction of infected humans over this same time, with individual instances in black and the average curve again in magenta (note that the y-axis here is an order of magnitude greater than that in Figure 4a).

4.3 Spatial Evolution of Outbreaks in Central Miami in Fall 2016

Figure 5 contains spatial outbreak data for a representative simulation instance of Figure 4. There is $n_s = 1$ seed node or index case chosen from the Central Miami population (shown in yellow). Data are shown at

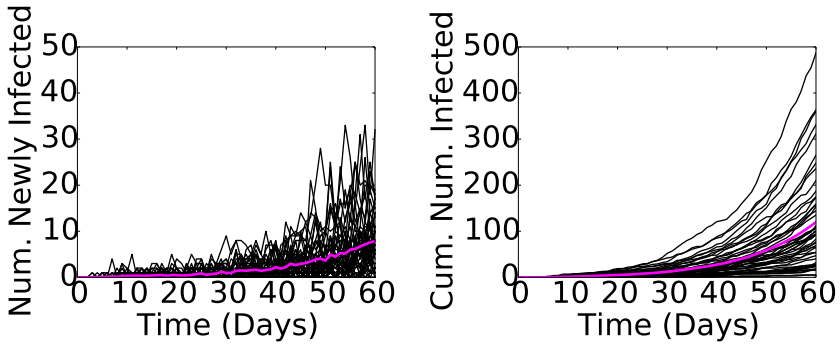

(a) (b)

Figure 4: Simulation data over the first two months of the Fall 2016, Central Miami Zika outbreak for a single index case (chosen uniformly at random) in each of 50 simulation instances. Seed nodes are selected from individuals in the Wynwood residential area of Central Miami, consistent with the actual outbreak. (a) Number of newly infected humans on each day. (b) Cumulative number of infected humans as a function of time. In both (a) and (b), the black curves are individual diffusion runs and the magenta curves are the time point-wise averages. After 60 days, the model predicts an average of 120 human cases of Zika, compared to the observed number of 120 cases.

$t = 20$, 40, and 60 days, respectively, for the three plots. The red dots indicate home locations of individuals that are, or have been, infected, and blue dots indicate their activity locations. Importantly, the right-most plot, corresponding to the spatial outbreak at $t = 60$ days, does not show a homogeneous distribution of infections. It shows significant numbers of infections for people living in Miami Beach (the peninsula on the far right). Fewer infections are predicted in the south-western region of the plots. These data (and data below) illustrate one difference between compartmental models and our HABM model: ODE models cannot provide this type of spatial detail in computed results.

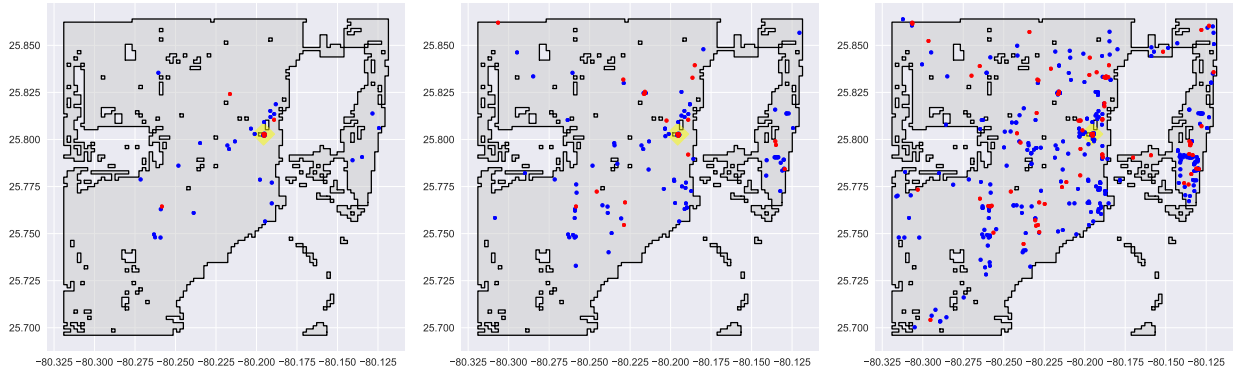

(a) $t = 20$ days. (b) $t = 40$ days. (c) $t = 60$ days.

Figure 5: Spatial distributions of home locations (red dots) and activity locations (blue dots) of all people infected with Zika by times $t = 20$, 40, and 60 days. This run produces 110 infections at 60 days, from one randomly chosen index case (in yellow) from the Wynwood area of Central Miami. The geographic region shown in these plots is Central Miami. Here, $\beta_{gh} = \beta_{hg} = 0.274$ and $n_s = 1$.

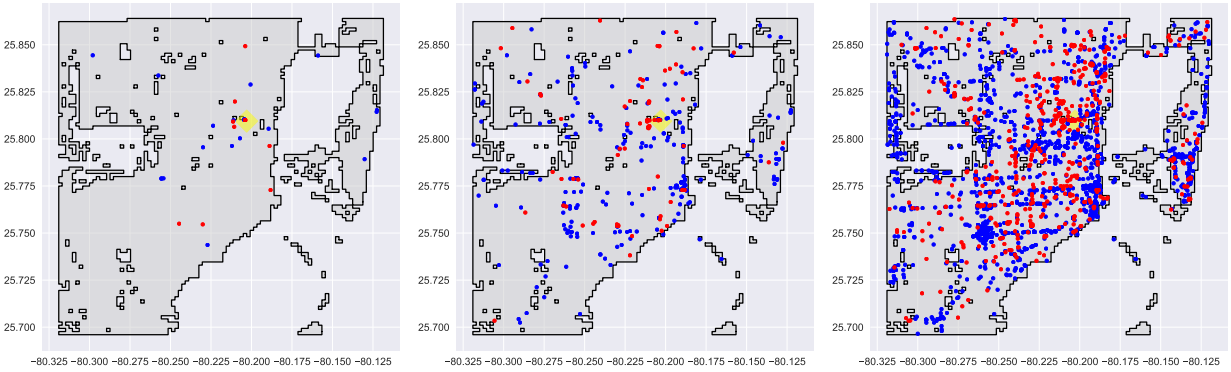

(a) $t = 20$ days. (b) $t = 40$ days. (c) $t = 60$ days.

Figure 6: Data for one randomly selected index case (yellow), chosen from the Wynwood area of Central Miami population, for more aggressive human-mosquito transmission. Red dots in the plots are home locations of people that get infected with Zika. Blue dots indicate locations that infected individuals visit. The geographic region shown in these plots is Central Miami. Here, $\beta_{gh} = \beta_{hg} = 0.36$, which is greater than the calibration value of 0.274, but still well within the range of values in Manore et al. (2014), and $n_s = 1$. The average outbreak size over all 50 runs is 709 people, which is greater than the 120 cases observed in Central Miami in Fall 2016. In this particular run, 746 people are infected in the first 60 days.

4.4 Spatial Spread of More Aggressive Zika With Larger $\beta = \beta_{gh} = \beta_{hg}$

Figure 6 provides an additional illustration of the types of benefits that an HABM affords over a compartmental model. These data are generated just as in the preceding figure, except that now $\beta = \beta_{gh} = \beta_{hg} = 0.36 > 0.274$. Each of the three plots shows the home locations of infected people (in red) and the other activity locations of these infected people (in blue), at $t = 20$, 40, and 60 days. At day-20, the home locations (red) and activity locations (blue) of infected individuals are scattered across the urban area of Central Miami. Then, at day-40, although the residential locations of infected individuals are still scattered across Central Miami, the activity locations cluster around the downtown area (25.775N, 80.187W) and Carol Way neighborhood (25.750N, 80.260W) as well as a couple of other regions. This clustering of activity locations implies that it is highly likely that individuals are infected by visiting these two locations. At day-60, more people get infected and the clustering phenomena of activity locations becomes even more apparent. Thus, HABM results aid in understanding how and where people get infected. Note that these location-based observations are not as apparent in Figure 5. This suggests, at least in some cases, that by increasing selected parameters to make an outbreak more pronounced, patterns of behavior may be more readily identified.

4.5 Illustrative Interventions

Figure 7 provides data for illustrative intervention scenarios. Transmission rates (in different colors) vary from 0.20 to 0.36, with solid curves corresponding to one index case and dashed curves corresponding to 10 initial cases. The results, while illustrative, nonetheless indicate the usefulness of models such as this one to assess intervention strategies to promote the public good.

5 SUMMARY

We introduce a novel hybrid agent-based model (HABM) to simulate vector-borne infectious diseases, such as Zika, by modeling each individual human as an agent and spatial regions of mosquitoes as compartments or gridcells. The HABM and compartmental model produce similar results in terms of macroscopic variables, such as the number infected individuals (epidemic curves). Due to the high resolution of our HABM, we

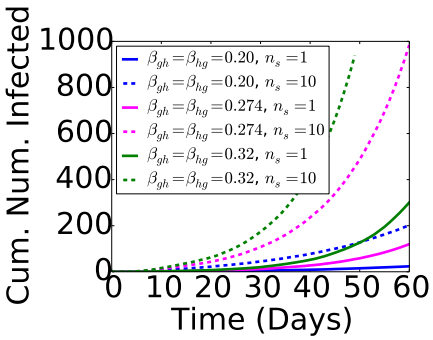

Figure 7: Interventions. The solid curves are baseline results with one index case. The corresponding dashed curve of the same color are for 10 index cases. All index cases are selected randomly from Wynwood. Colors correspond to different $\beta = \beta_{gh} = \beta_{hg}$.

discovered the clustering of activity locations of infected individuals, which we believe is the main cause of the spreading of the vector-borne infectious disease, for the conditions of the Miami outbreak.

There are several limitations of our work. The HABM does not account for seasonal variations in temperature, since we are primarily modeling the Zika outbreak over a 2-month window in the Fall 2016 in Miami. We also do not account for differences in other environmental factors (e.g., humidity and differential mosquito breeding grounds among the gridcells of Miami), which are discussed in Manore et al. (2015). However, such data can be included in the model, in the form of higher reproductive rates and mosquito population sizes in different regions of Miami. Mosquito mobility between gridcells is lacking, as is the use of measured numbers of mosquitoes. These are part of future work.

ACKNOWLEDGMENT

We thank the anonymous WSC reviewers for their helpful comments and recommendations. We thank our external collaborators and members of the Network Dynamics and Simulation Science Laboratory (NDSSL) for their suggestions and comments. We thank Bill Marmagas and the Compute Staff of the Biocomplexity Institute of Virginia Tech. This work has been partially supported by the NIH's National Institute of General Medical Sciences grants 5U01GM070694-13 and 1R01GM109718 as well as Defense Threat Reduction Agency Comprehensive National Incident Management System Contract HDTRA1-11-D-0016-0001.

REFERENCES

Barrett, C., R. Beckman, M. Khan, V. A. Kumar, M. Marathe, P. Stretz, T. Dutta, and B. Lewis. 2009. "Generation and Analysis of Large Synthetic Social Contact Networks". In *Winter Simulation Conference (WSC)*, edited by M. D. Rossetti, R. R. Hill, B. Johansson, A. Dunkin, and R. G. Ingalls, 1003–1014: Piscataway, New Jersey: Institute of Electrical and Electronics Engineers, Inc.

Bisset, K., J. Cadena, M. Khan, C. J. Kuhlman, B. Lewis, and P. A. Telionis. 2016. "An Integrated Agent-Based Approach for Modeling Disease Spread in Large Populations to Support Health Informatics". In *Inter. Conf. on Biomedical and Health Informatics*.

Brailsford, S. C., S. M. Desai, and J. Viana. 2010. "Towards the Holy Grail: Combining System Dynamics and Discrete-Event Simulation in Healthcare". In *Winter Simulation Conference (WSC)*, edited by B. Johansson, S. Jain, J. Montoya-Torres, J. Hugan, and E. Yucesan, 2293–2303: Piscataway, New Jersey: Institute of Electrical and Electronics Engineers, Inc.

Chahal, K., and T. Eldabi. 2008. "Applicability of hybrid simulation to different models of governance in UK healthcare". In *Winter Simulation Conference (WSC)*, edited by S. J. Mason, R. R. Hill, L. M?nch, O. Rose, T. Jefferson, and J. W. Fowler, 1469–1477: Piscataway, New Jersey: Institute of Electrical and Electronics Engineers, Inc.

Chouin-Carneiro, T., A. Vega-Rua, M. Vazeille, A. Yebakima, R. Girod, D. Goindin et al. 2016. "Differential Susceptibilities of Aedes aegypti and Aedes albopictus from the Americas to Zika Virus". *PLoS Neglected Tropical Diseases*:e0004543–1–e0004543–11.

Figueredo, G. P., P.-O. Siebers, M. R. Owen, J. Reps, and U. Aickelin. 2014. "Comparing Stochastic Differential Equations and Agent Based Modelling and Simulation for Early-Stage Cancer". *Plos One*:e95150–1–e95150–18.

Gu, W., and R. J. Novak. 2009. "Agent-based modelling of mosquito foraging behaviour for malaria control". *Transactions of the Royal Society of Tropical Medicine and Hygiene* 103:1105–1112.

Jindal, A., and S. Rao. 2017. "Agent-Based Modeling and Simulation of Mosquito-Borne Disease Transmission". In *16th Inter. Conf. on Autonomous Agents and Multiagent Systems (AAMAS)*.

Manore, C. A., K. S. Hickmann, J. M. Hyman, I. M. Foppa, J. K. Davis, D. M. Wesson, and C. N. Mores. 2015. "A Network-Patch Methodology for Adapting Agent-Based Models for Directly Transmitted Disease to Mosquito-Borne Disease". *Journal of Biological Dynamics* 9:52–72.

Manore, C. A., K. S. Hickmann, S. Xu, H. J. Wearing, and J. M. Hyman. 2014. "Comparing dengue and chikungunya emergence and endemic transmission in A. aegypti and A. albopictus". *Journal of Theoretical Biology* 356:174–191.

Mielczarek, B., and J. Zabawa. 2016. "Modeling Healthcare Demand Using a Hybrid Simulation Approach". In *Winter Simulation Conference (WSC)*, edited by T. M. K. Roeder, P. I. Frazier, R. Szechtman, E. Zhou, T. Huschka, and S. E. Chick, 1535–1546: Piscataway, New Jersey: Institute of Electrical and Electronics Engineers, Inc.

Perkins, T. A., A. S.Siraj, C. W. Ruktanonchai, M. U. Kraemer, and A. J. Tatem. 2016. "Model-based projections of Zika virus infections inchildbearing women in the Americas". *Nature Microbiology Letters* 1:1–7.

Schwarz, P., and E. Pruyt. 2016. "Modelling and simulation the Zika Outbreak under Deep Uncertainty: A Multi-Method Multi-Resolution Approach". In *34rd International System Dynamics Conference*.

Schweitzera, F., and D. Garcia. 2010. "An agent-based model of collective emotions in online communities". *European Physical Journal B* 77:533–545.

Sergon, K., C. Njuguna, R. Kalani, V. Ofula, C. Onyango, L. S. Konongoi, S. Bedno, H. Burke, A. M. Dumilla, J. Konde, M. K. Njenga, R. Sang, and R. F. Breiman. 2009. "Seroprevalence of Chikungunya virus (CHIKV) infection on Lamu Island, Kenya, October 2004". *Am J Trop Med Hyg* 78:333–337.

Viana, J. 2014. "Reflections on Two Approaches to Hybrid Simulation in Healthcare". In *Winter Simulation Conference (WSC)*, edited by A. Tolk, S. Y. Diallo, I. O. Ryzhov, L. Yilmaz, S. Buckley, and J. A. Miller, 1585–1596: Piscataway, New Jersey: Institute of Electrical and Electronics Engineers, Inc.

Zhang, Q., K. Sun, M. Chinazzi, A. P. y Piontti, N. E. Dean, D. P. Rojas, S. Merler, D. Mistry, P. Poletti, L. Rossi, M. Bray, M. E. Halloran, I. M. L. Jr., and A. Vespignani. 2017. "Spread of Zika virus in the Americas". *Proceedings of the National Academy of Sciences (PNAS)*.

AUTHOR BIOGRAPHIES

CHRIS J. KUHLMAN is a Research Scientist in the Biocomplexity Institute (BI) of Virginia Tech (VT). His e-mail address is ckuhlman@vt.edu.

YIHUI REN is a Post Doctoral Associate in the BI of VT. His email address is yren2@bi.vt.edu.

BRYAN LEWIS is a Research Associate Professor in the BI of VT. His email address is bryanlewis@bi.vt.edu.

JAMES SCHLITT is a Graduate Research Assistant in the BI of VT. His email address is jschlitt@bi.vt.edu.